

Transition to Bursting via Deterministic Chaos

Georgi S. Medvedev*

Department of Mathematics, Drexel University, 3141 Chestnut Street, Philadelphia, Pennsylvania 19104, USA
(Received 19 August 2005; published 27 July 2006)

We study statistical properties of the irregular bursting arising in a class of neuronal models close to the transition from spiking to bursting. Prior to the transition to bursting, the systems in this class develop chaotic attractors, which generate irregular spiking. The chaotic spiking gives rise to irregular bursting. The duration of bursts near the transition can be very long. We describe the statistics of the number of spikes and the interspike interval distributions within one burst as functions of the distance from criticality.

DOI: 10.1103/PhysRevLett.97.048102

PACS numbers: 87.19.La, 87.10.+e

Bursting oscillations are ubiquitous in the experimental and modeling studies of excitable cell membranes. Many models generating bursting have been subject to intensive research due to their physiological significance and dynamical complexity (see [1–7], and references therein). Under the variation of parameters, even minimal 3D models of bursting neurons exhibit a rich variety of periodic and aperiodic dynamical patterns corresponding to different spiking and bursting regimes. The transitions between these patterns may contain complex dynamical structures such as period-doubling (PD) cascades and deterministic chaos. In particular, it was shown that the transition from tonic spiking to bursting in a class of bursting neuron models, so-called square-wave bursters, contains windows of chaotic dynamics [1,5,7]. In the present Letter, we describe statistical features of the irregular bursting arising in a class of square-wave bursting models close to the transition from spiking to bursting. Prior to the transition to bursting, the systems in this class develop chaotic attractors, which generate irregular spiking. The chaotic spiking gives rise to irregular bursting (see Fig. 1). We analyze the statistics of the number of spikes and the interspike intervals (ISIs) within one burst.

To describe our results, we use a three variable model of a bursting neuron introduced in Ref. [2]. The model is based on three nonlinear conductances—persistent sodium I_{NaP} , the delayed rectifier I_K , a slow potassium M current I_{KM} , and a passive current I_L —and is representative for a class of square-wave bursters. The following system of three differential equations describes the dynamics of the membrane potential v and two gating variables n and w :

$$C\dot{v} = F(v, n, w), \quad (1)$$

$$\tau_n \dot{n} = n_\infty(v) - n, \quad (2)$$

$$\tau_w \dot{w} = w_\infty(v) - w, \quad (3)$$

where $F(v, n, w) = -g_{NaP}m_\infty(v)(v - E_{NaP}) - g_K n(v - E_K) - \gamma w(v - E_K) - g_L(v - E_L) + I$; g_s and E_s ($s \in \{NaP, K, L\}$) are the maximal conductance and the reversal potential of I_s , $s \in \{NaP, K, L\}$, respectively; and I is the

applied current. The maximal conductance of I_{KM} , γ , is viewed as a control parameter. The time constants τ_n and τ_w determine the rates of activation in the populations of K and KM channels. The steady state functions are defined by $s_\infty(v) = \{1 + \exp[(a_s - v)/b_s]\}^{-1}$, $s \in \{m, n, w\}$. The parameter values are given in the caption to Fig. 1.

The analysis of the bursting neuron models such as (1)–(3) uses a fast-slow decomposition [2,4,5]. Specifically, we note that the time constant τ_w presents the slowest time scale in the dynamics of (1)–(3). Therefore, we view $\alpha = \tau_w^{-1} > 0$ as a small parameter. In the limit as $\alpha \rightarrow 0$, system (1)–(3) is reduced to a 2D fast subsystem (1) and (2), where w is viewed as a parameter. The fast subsystem has a family of stable periodic orbits, which terminates at the homoclinic bifurcation at $w = w_{HC}$. A trajectory of the full system (1)–(3) approaches the surface foliated by the periodic orbits of the fast subsystem, S (Fig. 2). The evolution along S is governed by the slow equation (3), where the leading order approximation of $v(t)$ is obtained from the fast equations (1) and (2). When the trajectory hits the boundary of S (i.e., when $w > w_{HC}$), it jumps down to the curve of stable fixed points C , the only attracting set of

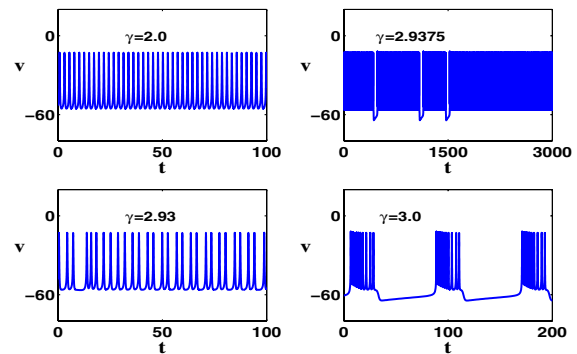


FIG. 1 (color online). Periodic and aperiodic firing patterns generated by (1)–(3) in the regimes close to the transition from spiking to bursting. The values of the parameters are $C = 1$ ($\mu\text{F cm}^{-2}$); $g_{Na} = 20$, $g_K = 10$, $g_L = 8$ (mS cm^{-2}); $E_{Na} = 60$, $E_K = -90$, $E_L = -80$ (mV); $a_m = -20$, $a_n = -25$, $a_w = -20$ (mV); $b_m = 15$, $b_n = 5$, $b_w = 5$; $\tau_n = 0.152$, $\tau_w = 20$ (ms^{-1}), and $I = 5$ pA.

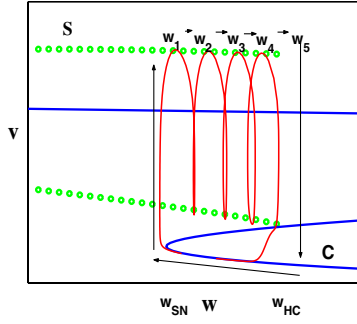


FIG. 2 (color online). The bifurcation diagram of the fast subsystem (1) and (2) with a superimposed periodic trajectory induced by the slow equation (3). Curves S and C indicate the families of periodic orbits and the fixed points, respectively.

the fast subsystem for $w > w_{HC}$. Then it evolves along C as shown in Fig. 2 until it reaches the boundary of C at $w = w_{SN}$, corresponding to a saddle-node (SN) bifurcation in the fast subsystem. This is followed by the jump back to S , and the oscillations in the fast subsystem resume. This description accounts for one cycle of bursting oscillation. Since the state of the fast system is determined by the value of the slow variable w , it is sufficient to know how w changes after each cycle of oscillations of the fast subsystem and after the period of quiescence:

$$w_{n+1} = P_\gamma(w_n), \quad n = 1, 2, \dots \quad (4)$$

This idea underlies the method of reduction of a class of models of bursting neurons to 1D maps proposed in Ref. [3]. In Ref. [3], we provided the analytical description for P_γ . It is a piecewise continuous map with the boundary layer I_0 corresponding to the homoclinic bifurcation in the fast subsystem (Fig. 3). There are two intervals of continuity in the domain of definition of P_γ , $I_1 = I^- \cup I^0$ and $I_2 = I^+$. The iterations of P_γ over I_1 correspond to the changes of w after each spike of voltage, and the definition of P_γ over I_2 captures the mechanism of return to spiking after the period of quiescence. In I_2 , $P_\gamma \approx w_{SN}$ is almost constant and can be well approximated by a linear function with a small negative slope [see remark 5.3(b) in Ref. [3]]. P_γ has a unique fixed point $\bar{w}_\gamma \in I_1$. For small values of γ , \bar{w}_γ is globally attracting. The trajectory of (4) stays in a small neighborhood of $\bar{w}_\gamma \in I_1$ after several iterations of P_γ . Therefore, the value of w in (1) and (2) changes little, and the fast subsystem generates periodic spiking. For increasing values of γ , the fixed point \bar{w}_γ loses stability through a PD bifurcation, giving rise to a stable period 2 orbit. Under further increase of γ , the numerical experiments show other PD bifurcations, and, eventually, the dynamics of the discrete system (4) becomes chaotic. This scenario fits well with the numerical results reported for related models [1,3]. While the maximum of P_γ over I_1 , $\bar{P}_\gamma = \max_{w \in I_1} P_\gamma(w)$, remains less than w_{HC} , $P_\gamma(I_1) \subset I_1$, the trajectories of (4) are trapped in I_1 . This means that,

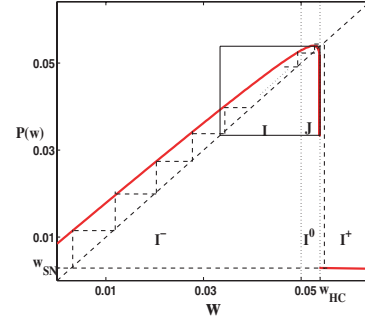


FIG. 3 (color online). The first return map for the slow variable w for the value of control parameter $\gamma = 2.9375$ close to the critical value γ^c .

in this regime, the continuous system exhibits spiking. The transition to bursting takes place at $\gamma = \gamma^c$: $\bar{P}_{\gamma^c} = w_{HC}$. For $\gamma > \gamma^c$, trajectories of (4) may leave I_1 . However, for values of γ just above γ^c , the window of escape J_γ is very small (see Fig. 3). Therefore, a trajectory of (4) with large probability spends a long time in I_1 before escaping to I_2 . If, in addition, the dynamics of (4) for $\gamma = \gamma^c$ has a mixing property, the transition to bursting lies through regimes of chaotic bursting with very long intervals of spiking appearing with large probability. Below, we study the statistics of the number of spikes and the ISIs within one burst for (1)–(3) near the transition to bursting.

Let $I = [w_0, w_{HC}]$, $w_0 = \lim_{w \rightarrow w_{HC}^-} P_\gamma(w)$ (see Fig. 3) and assume that at $\gamma = \gamma^c$ map $P_{\gamma^c}: I \mapsto I$ has an invariant probability measure μ absolutely continuous to the Lebesgue measure on I . In addition, we assume that P_{γ^c} has the mixing property:

$$\lim_{n \rightarrow \infty} \mu(A \cap P_{\gamma^c}^{-n}(B)) = \mu(A)\mu(B), \quad (5)$$

for all measurable sets $A, B \subset I$ [8]. Let $\gamma - \gamma^c > 0$ be sufficiently small. Denote $\delta = \mu(J_\gamma)$, where $J_\gamma = \{w \in I: P_\gamma(w) > w_{HC}\}$. Then the expected value (with respect to the probability measure μ) of the number of spikes within one burst is given by

$$N_\gamma = \mu(J_\gamma) + \sum_{k=2}^{\infty} k \mu_k, \quad (6)$$

where $\mu_k = \mu(P_\gamma^{-k+1}(J_\gamma) \cap \overline{\cup_{i=0}^{k-2} P_\gamma^{-i}(J_\gamma)})$ and \bar{A} stands for $I - A$. Let $m_k = \mu(\overline{\cup_{i=0}^{k-2} P_\gamma^{-i}(J_\gamma)})$ for $k \geq 2$. Then by mixing property (5), for sufficiently large $k_0 \in \mathbb{N}$,

$$\mu_k \approx \delta m_k \approx \delta m_{k_0} (1 - \delta)^{k-k_0}, \quad k > k_0. \quad (7)$$

The combination of (6) and (7) yields

$$N_\gamma = \Sigma_{k_0} + m_{k_0} \delta \sum_{k=1}^{\infty} (k + k_0) (1 - \delta)^{k-k_0}, \quad (8)$$

where Σ_{k_0} stands for the first k_0 terms on the right-hand side of (6). By taking into account $\Sigma_{k_0} = O(1)$ and

$\sum_{k=1}^{\infty} (k + k_0)(1 - \delta)^k = O(\delta^{-2})$, from (8) we obtain $N_{\gamma} = O(\delta^{-1})$. In a small neighborhood around the point of maximum, the graph of P_{γ} is to leading order quadratic. Therefore, the size of the window J_{γ} , $\delta = \mu(J_{\gamma}) = O(\sqrt{\gamma - \gamma^c})$, and $N_{\gamma} = O((\gamma - \gamma^c)^{-1/2})$. To estimate N_{γ} in a larger neighborhood of γ^c , we need to review certain facts about the structure of P_{γ} . It follows from the construction of P_{γ} in Ref. [3] that, outside of the exponentially small neighborhood of w_{HC} , \tilde{I} , P_{γ} can be approximated by a linear map. This implies that for $\gamma > \bar{\gamma} = \gamma^c + O(e^{-C_1/\alpha})$ the size of J_{γ} grows approximately linearly with γ , $\delta \approx O(\gamma - \bar{\gamma})$ and $N_{\gamma} = O((\gamma - \bar{\gamma})^{-1})$ for $\gamma > \bar{\gamma}$. Therefore, in the vicinity of γ^c , there are two regions of qualitatively distinct asymptotic behaviors of N_{γ} as a function of the distance from criticality. The numerical results shown in Fig. 4 confirm this conclusion and clearly indicate the boundary between these two regions, $\bar{\gamma} \approx 2.943$. The proposed mechanism for irregular bursting implies that, near the transition to bursting, N_{γ} has a geometric distribution, whose parameters are determined by the width of the window of escape J_{γ} (see Fig. 5).

Next we turn to estimating the expected value for the ISIs within one burst, T_{γ} . For small $\gamma - \gamma^c > 0$, we have

$$T_{\gamma} \approx \int_{I-J_{\gamma}} T(w, \gamma^c) d\mu(w), \quad (9)$$

where $T(w, \gamma)$ stands for the period of oscillations in the fast subsystem (1) and (2). By the Lebesgue-Besicovitch differentiation theorem [9], $\int_{J_{\gamma}} T(w, \gamma^c) d\mu(w) = O(\mu(J_{\gamma})) = O(\delta)$, for small $\gamma - \gamma^c > 0$. Since $\delta = O(\sqrt{\gamma - \gamma^c})$ for $\gamma \in (\gamma^c, \bar{\gamma})$, in this region, we have $T_{\gamma} = T_{\gamma^c} - O(\sqrt{\gamma - \gamma^c})$. To estimate T_{γ} for $\gamma > \bar{\gamma}$, we again use the proximity of P_{γ} to a linear map in $I - \tilde{I}$, which implies that $I - J_{\gamma} \approx (w_0, w_{\text{HC}} - O(\delta))$ and $d\mu(w) \approx C_2 dw$ in $I - \tilde{I}$ for some $C_2 > 0$. In addition, by the well known results of the bifurcation theory [10], $T(w, \gamma^c) \approx$

$T_0 - C_3 \log(w_{\text{HC}} - w)$, where positive constants T_0 and C_3 are independent from w , because the fast subsystem is close to a homoclinic bifurcation. Using these approximations and (9), we obtain $T_{\gamma} \approx C_2 \int_{w_0}^{w_{\text{HC}} - \delta} T(w, \gamma^c) dw \approx \bar{T} - C_4 \delta |\ln \delta| + O(\delta)$, where positive constants \bar{T} and C_4 are independent of δ and $\delta = O(\gamma - \bar{\gamma})$. The numerical results in Fig. 5 show that the asymptotic behaviors of T_{γ} are different for $\gamma < \bar{\gamma}$ and $\gamma > \bar{\gamma}$. The sublinear character of T_{γ} in the latter region is consistent with our estimate $T_{\gamma} - \bar{T} = O((\gamma - \bar{\gamma}) |\log(\gamma - \bar{\gamma})|)$.

Our analysis relies on the assumption that $P_{\gamma^c}: I \mapsto I$ is mixing. The latter is motivated by the structure of P_{γ^c} : the graph of P_{γ^c} has a very steep negative slope in the boundary layer adjacent to w_{HC} (Fig. 3). In fact, $P'_{\gamma^c}(w) = -\infty$ as $w \rightarrow w_{\text{HC}} - 0$ [3]. The presence of this very steep segment in the graph of the map, which must be involved in the system dynamics at the moment of transition to bursting, forms the basis for assuming mixing. Besides, our numerical results show a very good fit with the theoretically predicted statistics N_{γ} and, therefore, provide *a posteriori* justification for assuming that P_{γ^c} is mixing.

The map-based approach to bursting employed in this Letter reduces the problem of transition from spiking to bursting to the analysis of bifurcation scenarios in the families of 1D maps. The first event in these scenarios is the loss of stability of the fixed point corresponding to tonic spiking in the continuous system. For 1D maps, there are two codimension 1 bifurcations of fixed points: a SN and a PD bifurcation [10]. The bifurcation scenario described in Ref. [3] and in the present Letter originates from a PD bifurcation. A complementary mechanism of the transition to bursting is realized through a SN bifurcation (see Fig. 6). It has been recently demonstrated for a model for the leech heart interneuron [6] [see also remark 6.1(b) in Ref. [3]]. In analogy to the classification of excitability in spiking neuron models due to Rinzel and Ermentrout [5], we propose to distinguish mechanisms of the transition to bursting according to the underlying bifurcation mechanisms in the families of the first return maps: Type I transition is

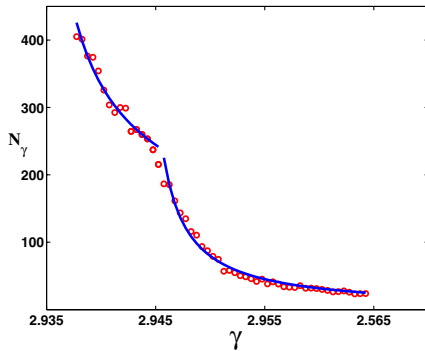


FIG. 4 (color online). The mean values of the number of spikes N_{γ} are fitted with $y = a(\gamma - \gamma^c)^{-1/2}$ ($\gamma < \bar{\gamma}$) and $y = b(\gamma - \gamma^c)^{-1}$ ($\gamma > \bar{\gamma}$), where $a \approx 25.42$, $b \approx 0.52$, $\gamma^c \approx 2.93419$, and $\bar{\gamma} \approx 2.934343$.

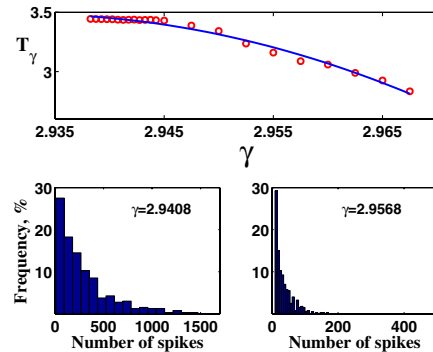


FIG. 5 (color online). The mean values of the ISIs within one burst T_{γ} and the histograms for the number of spikes within one burst.

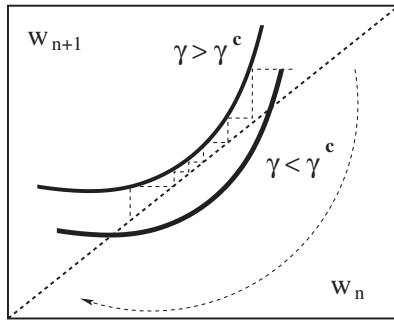


FIG. 6. The mechanism of the transition to bursting through a SN bifurcation. The SN bifurcation gives rise to a periodic orbit corresponding to a bursting solution. The global return mechanism is schematically indicated by the dashed arc.

realized via a SN bifurcation of the fixed point (which coincides with the global bifurcation of a periodic orbit; see Fig. 6); type II transition is realized through the disappearance (deflation) of the chaotic attractor preceded by a PD bifurcation. In both scenarios, the transition to bursting takes place after global bifurcations. However, the essential part of the bifurcation mechanism, which determines the traits of the bifurcating bursting patterns, in each case has a local character: a SN bifurcation in the type I scenario and the deflation of the chaotic attractor in type II. The principal difference between type I and type II transitions to bursting is that the latter necessarily involves irregular bursting whereas the former does not. In both scenarios, near the onset of bursting one finds patterns with duration of bursts, which can be extremely long. However, in the type I scenario these patterns are periodic, whereas in type II they are not. The number of spikes is constant for all bursts in type I models, and the ISIs have a small variance, but it goes to zero near the transition point. In contrast, both the number of spikes and ISI distributions in type II models exhibit significant variability. These observations agree well with the numerical results in Ref. [6] and in the present Letter. The asymptotic expressions for the number of spikes derived in the present Letter and in Ref. [6] have the same functional dependence on the distance from the transition point. However, it is important to note that in Ref. [6] this relation holds for the actual number of spikes, whereas in the present Letter this relation is derived for their mean values. The proposed classification requires certain structure of a differential equation model: (a) It should be a slow-fast system (b) with coexisting well-defined families of the periodic orbits and the fixed points in the fast subsystem. Under these assumptions, the mathematical analysis of bursting is most effective and they are considered to be standard. However, there are mechanisms for generating bursting that do not satisfy these assumptions. A small window of weakly chaotic bursting identified in Ref. [11] is an example of such a mechanism. In the

regime of chaotic bursting analyzed in Ref. [11], the width of the cylinder foliated by periodic orbits involved in bursting is comparable with the small parameter present in this system; i.e., condition (b) above does not hold (see Fig. 10 in Ref. [11]). This situation is not typical for slow-fast systems. In contrast, the mechanism for chaotic bursting of the present Letter retains the slow-fast character of the model and is qualitatively different from that in Ref. [11]. The mechanisms for the transition to bursting in neuronal models are reminiscent to those studied in the context of the transition to turbulence via intermittency [12]. In fact, the duration of (regular) bursting near the transition in the type I scenario and that of the laminar phases in the type I intermittency [13] share the same asymptotics due to the proximity to a SN bifurcation in both cases. In contrast, the statistical properties of the bursting patterns in the type II scenario are determined by the long intervals of irregular behavior and have not been studied before.

The author thanks Dr. Theo Geisel for useful suggestions. This work was partially supported by the National Science Foundation under Grant No. 0417624.

*Electronic address: medvedev@drexel.edu

- [1] T. R. Chay, *Physica (Amsterdam)* **16D**, 233 (1985).
- [2] E. M. Izhikevich, *Dynamical Systems in Neuroscience: The Geometry of Excitability and Bursting* (MIT, Cambridge, MA, 2006).
- [3] G. S. Medvedev, *Physica (Amsterdam)* **202D**, 37 (2005).
- [4] J. Rinzel, in *Proceedings of the International Congress of Mathematicians*, edited by A. M. Gleason (American Mathematical Society, Providence, 1987), pp. 135–169.
- [5] J. Rinzel and G. B. Ermentrout, in *Methods in Neuronal Modeling*, edited by C. Koch and I. Segev (MIT, Cambridge, MA, 1989).
- [6] A. Shilnikov and G. Cymbalyuk, *Phys. Rev. Lett.* **94**, 048101 (2005).
- [7] D. Terman, *J. Nonlinear Sci.* **2** 135 (1992).
- [8] Ya. G. Sinai, *Introduction to Ergodic Theory* (Princeton University, Princeton, NJ, 1976).
- [9] L. C. Evans and R. F. Gariepy, *Measure Theory and Fine Properties of Functions* (CRS Press, Boca Raton, FL, 1992).
- [10] J. Guckenheimer and P. Holmes, *Nonlinear Oscillations, Dynamical Systems, and Bifurcations of Vector Fields* (Springer, New York, 1983).
- [11] A. Shilnikov, R. Calabrese, and G. Cymbalyuk, *Phys. Rev. E* **71**, 056214 (2005).
- [12] L. D. Landau and E. M. Lifshitz, *Fluid Mechanics* (Butterworth-Heinemann, Oxford; Burlington, MA, 2003).
- [13] Y. Pomeau and P. Manneville, *Commun. Math. Phys.* **74**, 189 (1980).